Pressure-Temperature-Induced Transformations of Hydrocarbon-Fluorocarbon Mixtures into Nano- and Micron-Size Diamonds

Valery A. Davydov[1], Viatcheslav Agafonov[2], Valery N. Khabashesku[3,4*]

[1]L.F. Vereshchagin Institute for High Pressure Physics of the RAS, Troitsk, Moscow, Russia
[2]GREMAN, UMR CNRS-7347, Université F. Rabelais, Tours, France
[3]Department of Chemical and Biomolecular Engineering, University of Houston, USA
[4]Center for Technology Innovation, Baker Hughes, a GE Company, Houston, TX, USA

Article info

Received:
10 June 2016

Received in revised form:
28 October 2016

Accepted:
25 January 2017

Abstract

Studies of thermal transformations of naphthalene ($C_{10}H_8$), fluorographite ($CF_{1.1}$) and octafluoronaphthalene ($C_{10}F_8$) and their binary mixtures ($C_{10}H_8$ – $CF_{1.1}$, $C_{10}H_8$ – $C_{10}F_8$) under pressure of 8 GPa have been undertaken as models for gaining understanding of processes of carbonization, graphitization and diamond formation in pure hydrocarbon, fluorocarbon and carbon-hydrogen-fluorine-containing systems under high pressures. The studies found a significant reduction in the initiation temperature thresholds for all major thermal transformation processes in case of binary mixtures with respect to thresholds for pure hydrocarbon and fluorocarbon compounds. Another distinctive feature of the transformations of binary mixtures with respect to diamond formation stage of the transformations of pure hydrocarbons, has been the presence of massive quantity of nanosize (10–60 nm) diamond fraction in the products from binary mixtures along with the micron-size (5–20 μm) diamond fraction, typically observed in the transformations of pure hydrocarbons. The origin of nanodiamond was related to the specifics of carbonization of fluorocarbon compounds under pressure, which at 800–1000 °C produces, along with submicron particles of graphite-like material, a significant amount of closed shell 2–5 layer carbon nanoparticles of 5–15 nm size. These onion-like carbon nanoparticles act as precursors for formation of nano size diamond fractions in the transformations of binary mixtures of hydrocarbon and fluorocarbon compounds. These results potentially open a new direction for metal catalyst-free synthesis of pure and doped diamonds for broad applications. The present article gives an overview of this emerging area of research.

1. Introduction

The industrial applications of diamond are enabled by its unique material properties, the highest hardness and thermal conductivity of any known bulk material, the lowest coefficient of thermal expansion, chemical inertness and wear resistance, low friction, electrically insulating and optically transparent from UV to far infrared region [1]. The global market for natural diamonds, mined mostly in Russia, Canada, Australia and Africa, has been estimated at $80 billion in 2014. However, it recently showed the declining trend caused by lowering demand for gem-quality diamonds and higher mining costs due to deeper mines and their more remote location. In comparison, the market for synthetic diamond is expected to grow from $15.7 billion in 2014 to $28.8 billion in 2023 at average rate of 7% per year [2]. The synthetic diamonds are already more affordable than natural, and over time their production cost and value are expected to reduce further.

The first reproducible synthesis of diamond, reported in 1953 in Sweden, was followed in 1954–1955 in USA by Hall and Bundy at GE company and in Soviet Union by Vereshchagin et al.

*Corresponding author. E-mail: valery.khabashesku@bhge.com

© 2017 Al-Farabi Kazakh National University

The main manufacturing technologies for synthetic diamond currently involve (i) high pressure-high temperature (HPHT) process which recreates conditions of natural growth deep inside the Earth, (ii) low pressure chemical vapor deposition (CVD) from carbon plasma directed over a substrate at 700–900 °C, using methane/hydrogen mixture as feedstock, mostly for polycrystalline coatings, and single crystals of diamond a few millimeters in size, (iii) explosive synthesis, developed in USSR in 1960s and commercially used since late 1990s for producing nanodiamonds (~5 nm diameter) through detonation of carbon-containing explosives, e.g., TNT. Among these technologies, HPHT process is widely used because of its relatively low cost. The process uses graphite as a feedstock. The challenge in converting graphite into diamond rests on that diamond is thermodynamically less stable than graphite by $\Delta H° = 1.897$ kJ/mol. However, it is separated from graphite by a barrier of 31.84 kJ/mol which makes diamond stable kinetically. To overcome this barrier, Co, Ni or Fe metals, are admixed to graphite powder, to act as "solvent-catalysts" at temperatures and pressures above 1500 °C and 5 GPa, respectively.

Diamonds, produced by this process, always contain metal impurities presence of which can be detrimental for some applications, for example, heat sink applications in electronics. Therefore, the attempts on metal catalyst-free synthesis of diamond were undertaken and reported as early as 1963 by Bandy [3], later followed by Vereshchagin et al. [4]. These reported processes, although successful, were run however under severe conditions, pressure as high as 12 GPa and temperature as high as 3000 °C, applied to graphite feed in a high pressure cell. Need for a milder industrially viable process conditions became a driver for HPHT studies on diamond precursors other than graphite.

The most common hypothesis for origin of diamond in nature is from direct conversion of organic carbon under high-pressure conditions in the Earth's interior. The discovery of diamondoids, the smallest nanodiamond structures found in mature high-temperature hydrocarbon oil [5], suggests a possible existence of chemical pathway to diamond from hydrocarbons, serving as carbon source.

2. HPHT synthesis of diamond from hydrocarbons

Thermal decomposition of solid hydrocarbons with different molecular structures and bonding types of carbon occurring under a pressure of 8 GPa and temperature of 1500 °C was studied in details in a series of works [6–11]. It was particularly shown that naphthalene, an aromatic hydrocarbon, $C_{10}H_8$, when compressed at 8 GPa for 1 min completely converts into diamond at temperature as low as 1300 °C through a catalyst-free process [9]. It was also observed [10] that when graphite is in contact with the naphthalene it also transforms into diamond without a catalyst under the same mild P-T conditions, 8 GPa and 1300 °C. The fact that the temperature for diamond formation from hydrocarbons in the P-T region of thermodynamic stability of diamond is significantly lower that the temperature for direct transformation of graphite into diamond [3, 4] can be explained by activation energy being considerably lower for thermal destruction of hydrocarbons as compared to graphite which possesses a crystalline frame highly resistant to thermal treatment [7]. However, the finding that introduction of chemically bonded hydrogen (e.g., in the form of naphthalene, $C_{10}H_8$) into reaction zone filled with the graphite to an overall hydrogen-to-carbon atomic ratio of 1:8 can cause such drastical drop in the process parameters of transformation of graphite into diamond did not seem trivial. The proposed mechanism assumed that hydrogen or gaseous hydrocarbon products of degradation of naphthalene at least partially can remain in the reaction zone up to temperature of 1300 °C and participate in the transformation of graphite into diamond either through deformation of crystalline frame of graphite by intercalation or its chemical splitting followed by chemical transport of carbon [11]. To find out whether another chemical element besides hydrogen can benefit the HPHT synthesis of diamond, the closest to hydrogen element, such as is fluorine, was considered since it forms a variety of fluorocarbon compounds including gaseous ones. Therefore, the experimental studies [12–15] have been carried out with the objective to evaluate the effect of fluorine in fluorocarbons on conditions for HPHT synthesis of diamond. The fluorocarbon compounds used in these studies were fluorographite $CF_{1.1}$ and octafluoronaphthalene $C_{10}F_8$ in the form of refined white-colored powders. Naphthalene with the impurity content less than 0.5% was used as a hydrocarbon model compound. For thermobaric treatment and subsequent studies pure fluorographite $CF_{1.1}$ and octafluoronaphthalene, as well as their homogeneous mixtures with naphthalene of different proportions were used.

3. Crystallization of carbon products of thermal decomposition of pure fluorographite $CF_{1.1}$ and naphthalene under pressure of 8 GPa

For creation of high pressure and high temperature a methodology described in works [7–11] was applied. Cylinder-shaped samples (4.5 mm diameter and 3 mm height), prepared by pressing at room temperature, were inserted into graphite container and then placed into a high pressure chamber of "Toroid" type. The container also served as a heater of the samples. The natural material, called "katlinite", served both as pressure transmitting media and electrical and thermal insulator having no direct contact with the sample. The experimental procedure consisted in loading the high pressure apparatus to 8 GPa at room temperature, then heating of the sample to the desired temperature (with an average heating rate of about 50 °/sec) followed by isothermal exposure of the sample at this temperature during a given time (t = 20 sec). High pressure treated samples have been isolated by quenching to room temperature under pressure and then after complete pressure release. The recovered samples have been characterized by X-ray diffraction, fluorine content and weight loss after thermobaric treatment of the samples. X-ray diffraction patterns of powder samples have been recorded on INEL CPS 120 diffractometer using $CoK_{\alpha 1}$ radiation source. Microscopy characterization of the samples was carried out on scanning electron microscope (SEM) and transmission electron microscope (TEM).

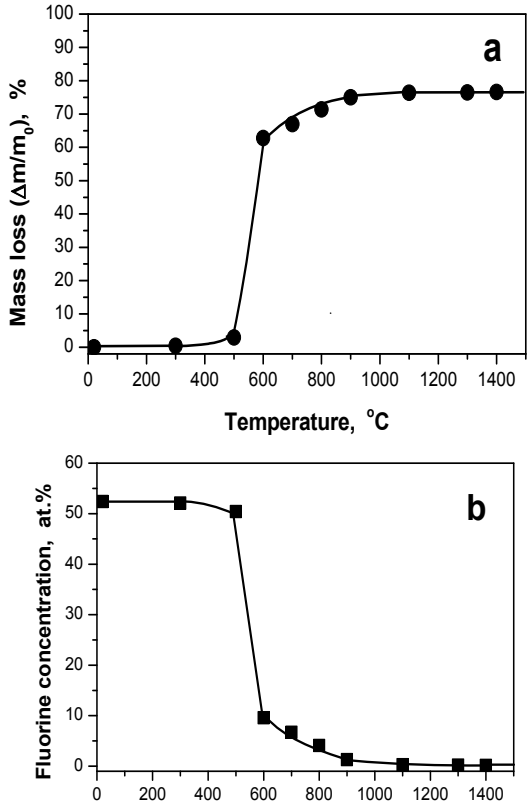

Fig. 1. Mass loss (a) and fluorine content (b) in $CF_{1.1}$ samples measured after their heating at 8 GPa for 20 sec vs. heating temperature.

Thermal stability studies data of fluorographite under pressure of 8 GPa are represented by Fig. 1a which shows the plot of mass loss by HPHT treated $CF_{1.1}$ samples vs. temperature of heating. Samples have been weighed with their graphite containers both before and after thermobaric treatment. Graphite containers usually maintained their integrity after the experiments. If $CF_{1.1}$ samples have lost fluorine only in the form of gaseous F_2, the theoretically expected mass loss would be 73.6%. However, the experimental value of Δm/m reaches saturation at 900 °C and equals to 76.6%. Figure 1b shows plot of fluorine content in the HPHT treated $CF_{1.1}$ samples vs. temperature of heating. Most of fluorine loss by the sample takes place in the temperature range of 500–700 °C. The sample, heated to 900 °C, contained virtually no fluorine (just 0.29 at.%).

Given these data and results of previous studies by variable temperature-mass spectrometry of gaseous products of decomposition of $CF_{1.1}$ at temperatures up to 1000 °C where no F_2 but CF_4 and C_2F_6 were detected, the transformation of $CF_{1.1}$ can be described by the following equation: $CF_{1.1} \rightarrow C_{0.64} + C_{0.36}F_{1.1} \uparrow$ (gaseous fluorocarbons: CF_4, and C_2F_6).

X-Ray studies show that the diffractograms of samples, treated at temperatures below 600 °C, are similar to starting $CF_{1.1}$ by lacking narrow diffraction peaks (Fig. 2) which indicate a predominance of amorphous phase. In this temperature range, the increase of T results in the intensity decrease of amorphous component and appearance (at 600 °C) on its background of 002 and 10 peaks which are characteristic of two-dimensional carbon (Fig. 2). The intensity of these peaks at 600 °C is low.

The diffractograms of samples, produced at temperatures of 600, 800, 900, 1100, and 1400 °C, are shown on Fig. 2. They clearly show that already at 900 °C the presence of three-dimensional carbon (graphite) in the carbon products is predominant.

Figure 3 shows comparison of changes in the interplanar distance d_{002} for carbon materials obtained by thermal degradation of naphthalene with

regard to temperature. The top dashed line on Fig. 3 corresponds to d_{002} distance at which the 10 diffraction peak of two-dimensionally ordered carbon splits up and shows a 100 and 101 peaks, typical for graphite. The bottom dashed line corresponds to a theoretical d_{002} distance in ideal graphite. The interesting fact that can be learned from this figure is that in spite of a shorter time of thermal treatment than in experiments with naphthalene, thermal decomposition of $CF_{1.1}$ produces a graphite with d_{002} distance close to an ideal value already at temperatures as low as 900 °C.

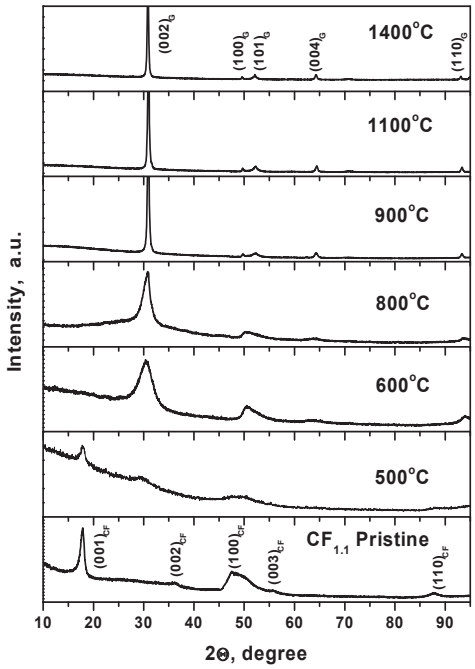

Fig. 2. XRD patterns of pristine $CF_{1.1}$ and products of its treatment under pressure of 8 GPa and different temperatures.

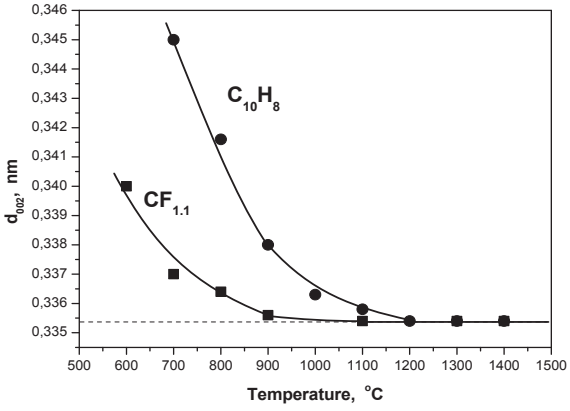

Fig. 3. Temperature dependence of interlayer distance (d_{002}) in the packings of graphene planes formed through graphitization of carbon residue resulting from carbonization of $CF_{1.1}$ and $C_{10}H_8$ at 8 GPa.

Figure 4a presents an exciting SEM image of the crystallites of graphite formed from $CF_{1.1}$ under pressure of 8 GPa and temperature of 1000 °C. This image shows graphite crystallites which possess an uncommon, surprisingly clear hexagon-faceted morphology not been observed previously. For example, graphite crystals, obtained by thermal decomposition of naphthalene and other solid hydrocarbons, appear as oval-shaped plateletts having curved edges (Fig. 4b). The difference in morphology of the crystallites shown on Figs. 4a and b points at differences in the chemical effect of arising gas environment on carbon crystallization during thermal decomposition of $CF_{1.1}$ and $C_{10}H_8$ at 8 GPa. At the same time, these studies have shown that unlike naphthalene, thermal treatment of $CF_{1.1}$ at 8 GPa does not result in formation of diamond up to temperature of 1500 °C. Possible reason for that is substantial difference in size and chemical nature of fluorine and hydrogen atoms leading to structure perturbation of graphite-diamond transition layer, which is essential for diamond growth by this mechanism in a hydrocarbon system where hydrogen is replaced by fluorine [16].

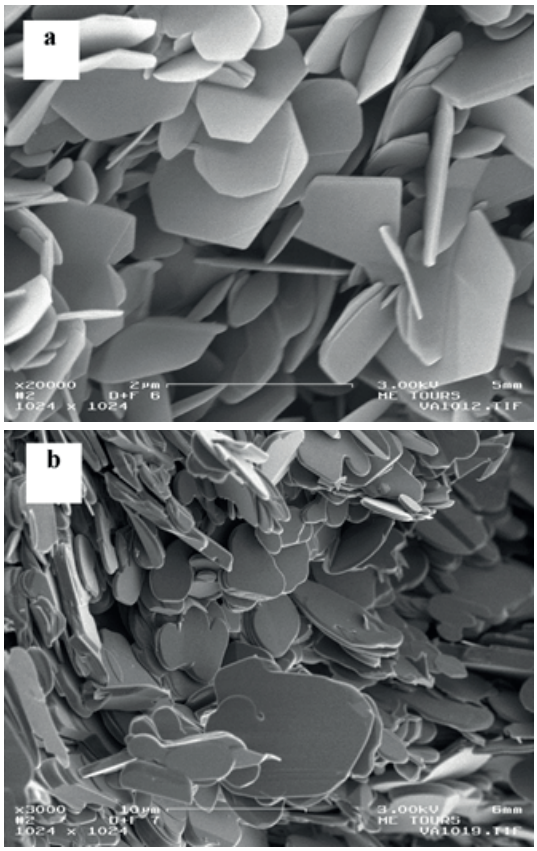

Fig. 4. Comparison of SEM images of graphite platelets obtained by decomposition of $CF_{1.1}$ at 8 GPa and 1000 °C for 20 sec (a), and naphthalene $C_{10}H_8$ at 8 GPa and 1200 °C for 20 sec (b).

4. Thermal transformations of homogeneous mixtures of $CF_{1.1}$ and naphthalene at 8 GPa

Evolution of XRD patterns of products resulting from treatment of homogeneous mixture of $CF_{1.1}$ and naphthalene (with mass ratio $CF_{1.1}$: $C_{10}H_8$ = 1:1) under pressure of 8 GPa and variable temperatures can be observed on Fig. 5. SEM images of samples produced by treatment of this binary mixture at different temperatures are shown on Figs. 6 and 7. These data have shown that active stages of carbonization processes in binary mixtures of $CF_{1.1}$ with naphthalene involve release of fluorine and hydrogen, and subsequent structural assembling of carbon residues. They proceed at significantly lower temperatures than in cases of neat $CF_{1.1}$ and naphthalene. This can be clearly noticed by comparison of XRD patterns of products resulting from treatment at 8 GPa and 500–600 °C of $CF_{1.1}$ (Fig. 2), naphthalene [11] and their binary mixtures (Fig. 5).

According to data presented on Figs. 2 and 3, fluorographite $CF_{1.1}$ converts at 500 °C into a material which is produced at initial stages of carbonization of $CF_{1.1}$. Significant part of this material is still comprised of $CF_{1.1}$ whose major reflections dominate the XRD pattern of the sample produced at 500 °C. Fluorine loss is less than 10% at this temperature. The content of graphitizing carbon residue, which is built from nanosize packings of graphene layers witnessed by appearance of broad feature near 29°, is also not higher than 10%. In the products of naphthalene transformation at 8 GPa and 500–600 °C, formation of packing of graphene layers is not observed at all.

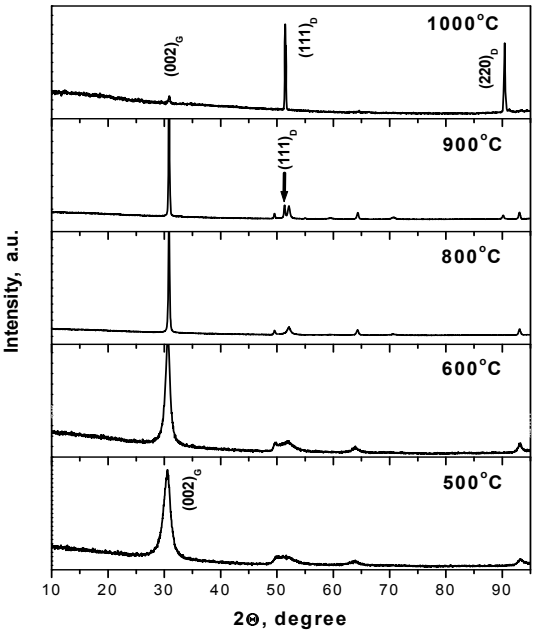

Fig. 5. XRD patterns of samples produced by treatment of homogeneous mixtures of $CF_{1.1}$ and naphthalene (with mass ratio $CF_{1.1}$: $C_{10}H_8$ = 1:1) under pressure of 8 GPa and variable temperatures.

Unlike neat $CF_{1.1}$ and naphthalene, their binary mixture of 1:1 mass ratio undergoes convertion at 500 °C into a carbon material made of packings of graphene layers (Fig. 5), similar to the product formed from pure $CF_{1.1}$ and naphthalene at temperatures higher than 800 °C. Difference in morphologies of the products of transformation of neat $CF_{1.1}$ and binary mixture of $CF_{1.1}$ with naphthalene were noticed. The material resulting from treatment of $CF_{1.1}$ represents an agglomerate of small particles lacking any particular morphological features, while the material obtained from binary mixture (Fig. 6a) forms a separate flakes typical for layered graphene packings. Such significant difference in formation temperature for the same carbon states points at dissimilarities in the mechanisms of carbonization of neat hydrocarbon and fluorocarbon compounds and their binary mixtures. Drop of graphitization temperature threshold for $CF_{1.1}$ and naphthalene in binary mixtures, noted in works [12–15], has been related to difference between purely thermal and combined thermochemical mechanisms of carbonization of fluorocarbon and hydrocarbon compounds. The obtained results led to conclusion that the processes of defluorination and dehydrogenation of neat $CF_{1.1}$ and naphthalene, respectively, are mainly thermally activated. In case of binary mixtures, there appears to be an additional thermochemical channel for processes of carbonization of both components of the mixture which involves an active fluorine-hydrogen chemical interaction leading to thermodynamically favorable formation of HF molecules and therefore requiring lower activation energy. The outcome of this mechanism is effective drop of temperature threshold for graphitization of carbon residue produced by carbonization of $CF_{1.1}$ and naphthalene binary mixtures. The emergence of 3D ordering of packings of graphene layers and formation of graphite is indicated in XRD by a modulation of 2D (10) reflection near 50°, which in case of binary mixture becomes observable after treatment already at temperature of 600 °C (Fig. 6b).

Treatment of binary mixture at 600 and 800 °C produces graphite materials which form crystals with the degree of perfection increasing with temperature (Figs. 6b and c). As SEM images show, consistent elevation of treatment temperature is

followed by gradual increase of lateral size and thickness of graphite crystallites. According to Fig. 6d, lateral size of graphite particles at temperature of 900 °C can reach 5–10 micron. Along with graphite, formation of diamond is also observed at this temperature. Appearance of submicron and micronsize diamond crystals is presented on Fig. 6d. At treatment temperatures higher than 1000 °C, diamond becomes a major component of the products of transformation of binary mixture of $CF_{1.1}$ with naphthalene (Figs. 6e and 7). Although formation of diamond has been observed for all studied compositions of binary mixtures of $CF_{1.1}$ with naphthalene, the content of diamond fraction in the transformation products obtained under the same treatment temperature depends on atomic F/H ratio in the starting mixture. In the series of experiments on different mixture compositions of $CF_{1.1}$ and naphthalene with atomic F/H ratios of 1:1, 1:2, 1:3, 1:7, and 1:10, carried out at 8 GPa and temperature of 1000 °C, maximum (100%) yield of diamond was observed for mixtures with F/H ratio equal to 1:7.

It should be noted that the observed temperature threshold (900 °C) for formation of diamond from binary mixture of $CF_{1.1}$ and naphthalene is significantly lower than the initial temperature of diamond formation from naphthalene and other aromatic hydrocarbons, where it was found to be about 1300 °C at 8 GPa.

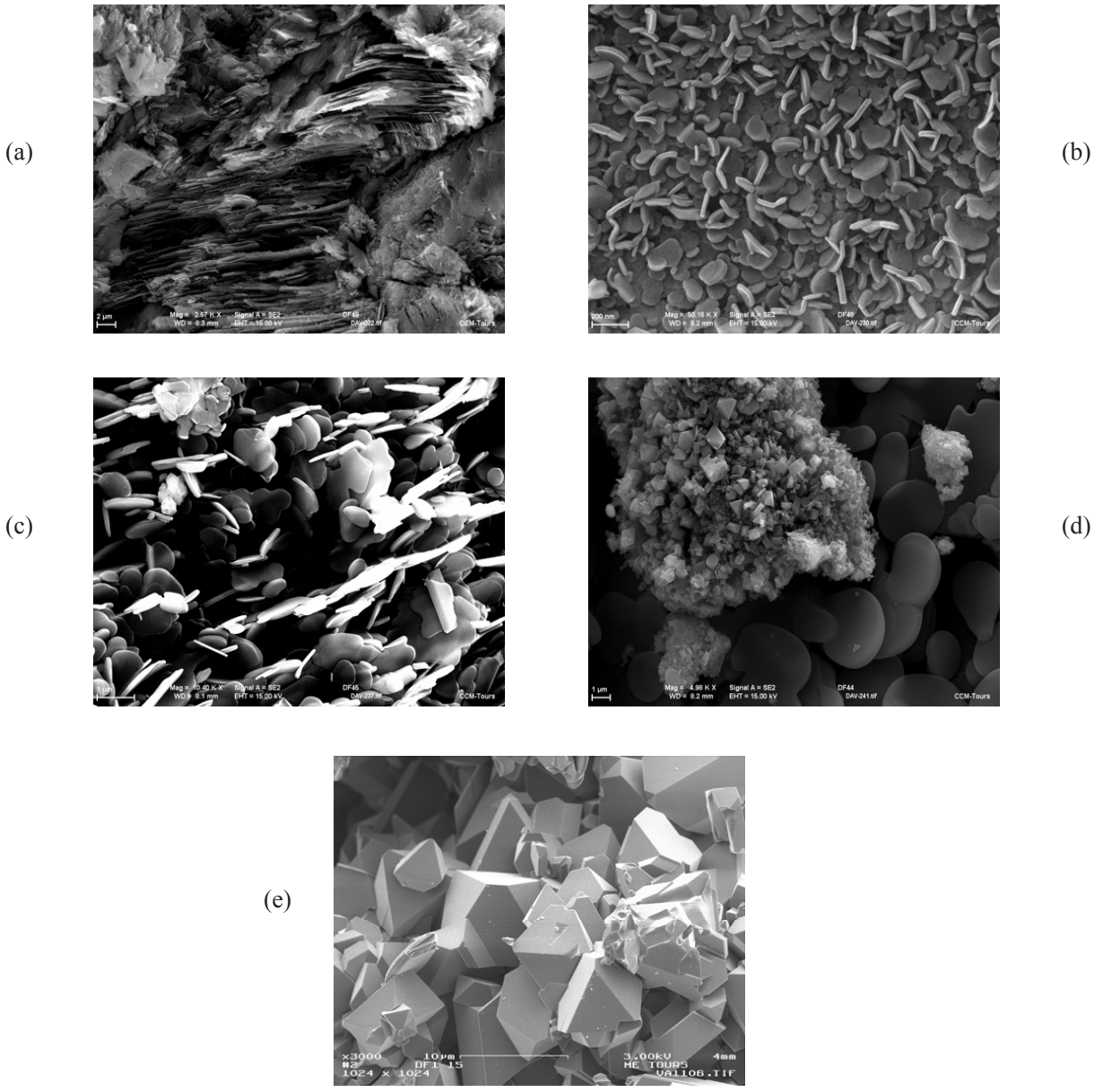

Fig. 6. SEM images of samples produced by treatment of 1:1 homogeneous mixtures of $CF_{1.1}$ with naphthalene at pressure of 8 GPa and different temperatures: 500 °C (a), 600 °C (b), 800 °C (c), 900 °C (d), and 1100 °C (e).

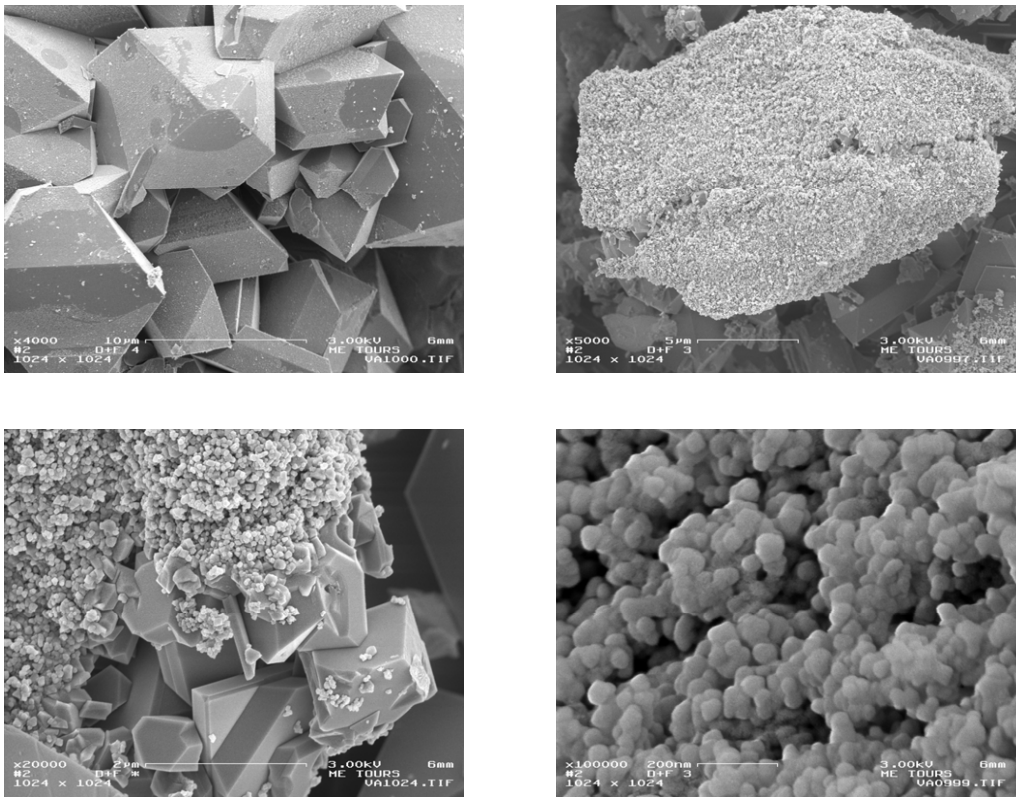

Fig. 7. SEM images of diamonds produced by treatment of 1:4 homogeneous mixtures of $CF_{1.1}$ with naphthalene at pressure of 8 GPa and temperature of 1000 °C.

Figure 7 shows SEM images of diamonds produced by treatment of homogeneous mixtures of $CF_{1.1}$ with naphthalene at 1:4 mass ratio under pressure of 8 GPa and temperature of 1000 °C. The observed diamond fraction mainly consists of well-faceted crystals predominantly shaped into octahedra with linear sizes in the range of 0.5–15 microns (Fig. 7a). Formation of diamonds of this type is characteristic for processes of high pressure thermal transformations of naphthalene and other hydrocarbons [10]. However, the distinctive feature of transformation of binary mixture of $CF_{1.1}$ and naphthalene is that in this case along with bulk microscale size crystals the nanosize diamond fraction is also formed (Fig. 7b and c). This fraction looks on SEM image like a uniform mass of discrete particles sized in the 10–60 nm range and lacking a well-defined crystalline form (Fig. 7d). Nevertheless, it is interesting to note that according to TEM images shown on Fig. 8 many of these diamond nanoparticles with linear sizes as small as 14–20 nm already demonstrate a clearly featured crystal faces in the form of octahedra, truncated octahedra, and twinned hexagonal plates.

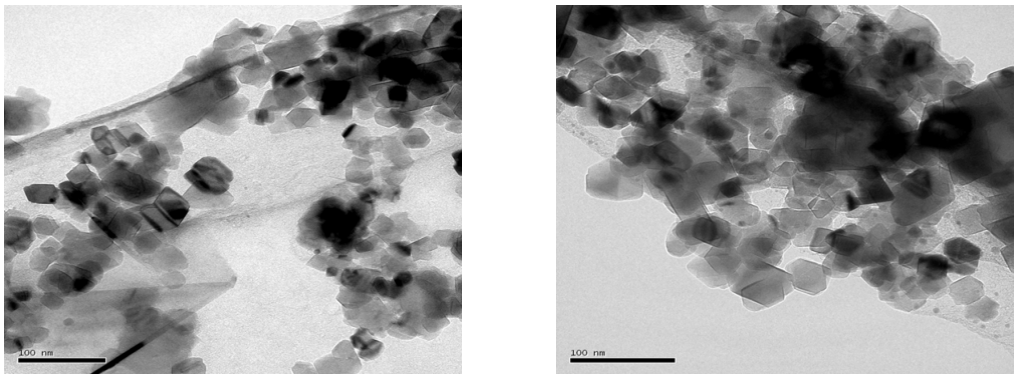

Fig. 8. TEM images of nanosize diamond crystals produced by treatment of 1:4 homogeneous mixtures of $CF_{1.1}$ with naphthalene under pressure of 8 GPa and temperature of 1000 °C.

The obtained results clearly show that thermal transformations of homogeneous mixtures of $CF_{1.1}$ with naphthalene under high pressures are characterized by substantial decrease of graphitization temperature of carbonization products obtained from both components of the mixture. Also, there is a substantial decline of initial temperature threshold for diamond synthesis as compared to pure hydrocarbon growth systems. The observed reduction of diamond synthesis temperature in binary systems of $CF_{1.1}$ and naphthalene in comparison with pure naphthalene can be explained by synergistic effect of fluorine-hydrogen chemical interaction on carbonization processes enabling the graphitization of carbon residues to proceed at lower temperature.

5. High-pressure carbon states from HPHT treatment of naphthalene, octafluoronaphthalene and their homogeneous and "heterogeneous" mixtures

The observed large scale formation of nanosize diamond fraction along with the micron-size diamond fraction under HPHT transformations of binary mixtures of $C_{10}H_8 - CF_{1.1}$ led to attempted consideration of possible existence of size-dependent relationship of fractional composition of diamond products on fractional composition of carbonization products, acting as direct precursors for diamond formation under conditions of binary mixtures. The objective was to follow a "genetic" relationship between carbonization products and one of the two components of starting binary mixture. In order to minimize a possible input of structural differences in the initial hydrocarbon and fluorocarbon compounds to the specifics of their transformation reactions, two structural analogues, naphthalene ($C_{10}H_8$) and octafluoronaphthalene ($C_{10}F_8$), have been selected as model compounds for this study.

Samples of pure $C_{10}H_8$, $C_{10}F_8$ and homogeneous $C_{10}H_8 - C_{10}F_8$ mixtures in the form of tablets (diameter 5 mm, height 4 mm) were obtained by cold-pressing of starting materials. Given the difficulty of unambiguous assignment of carbonization products to one of the starting components under conditions of homogeneous binary mixture, in this work we have also studied the transformations of so-called "heterogeneous" $C_{10}H_8 - C_{10}F_8$ mixtures. These samples represented a bilayer compacts composed of two separate compressed tablets of naphthalene and octafluoronaphthalene with the diameter of 5 mm and height of 2 mm each.

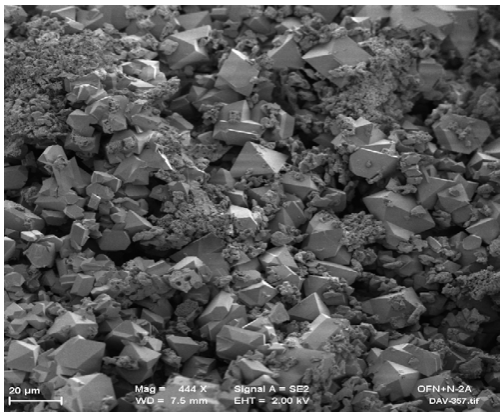

Fig. 9. SEM image of diamond material obtained by treatment of homogeneous mixture of $C_{10}H_8 - C_{10}F_8$ at 8 GPa and 1100 °C.

From methodology point of view, this work is a comparative study of high-pressure states resulting from treatment of naphthalene, octafluoronaphthalene and their homogeneous and "heterogeneous" mixtures under the same pressure, temperature and time of isothermal exposure. X-Ray diffraction analysis of transformation products of pure $C_{10}H_8$, $C_{10}F_8$ and homogeneous $C_{10}H_8 - C_{10}F_8$ mixtures at 8 GPa and different temperatures has shown a significant decline in temperature threshold for the initiation of carbonization, graphitization and formation of diamond under conditions of binary mixture as compared to pure $C_{10}H_8$ and $C_{10}F_8$. For instance, the initiation temperature for diamond formation from homogeneous $C_{10}H_8 - C_{10}F_8$ binary mixture was ~1000 °C, which is 300 °C below a similar parameter for naphthalene. At 1100 °C, a virtually 100% conversion of carbonization products of binary mixture into diamond is observed. In this case, according to SEM image shown in Fig. 9, diamond product presents a mixture of nano- and micron-size fractions of diamond.

To find out the origin of nano- and micron-size fractions of diamond, the carbon materials produced by transformations of $C_{10}H_8$ and $C_{10}F_8$ in the contact layer of the sample of heterogeneous $C_{10}H_8 - C_{10}F_8$ mixture at temperatures of 900–1000 °C, which are near the temperature threshold for diamond formation, have been studied. SEM images of transformation products of naphthalene and octafluoronaphthalene, taken in a contact region of heterogeneous sample of binary mixture treated at 8 GPa and 1000 °C, are shown on Fig. 10.

According to Fig. 10a, main products of transformation of naphthalene under these conditions are graphite (~85%) and diamond (~15%) particles with the average sizes of ~5 μm. In comparison, the transformation product of octafluoronaphthalene

(a) 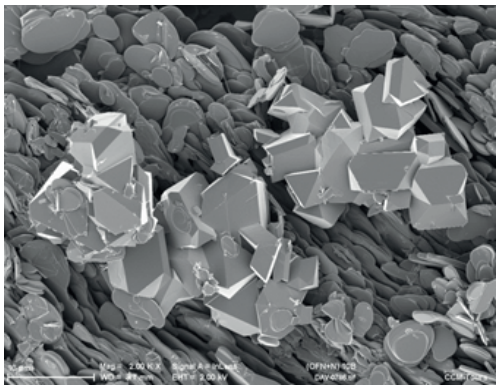 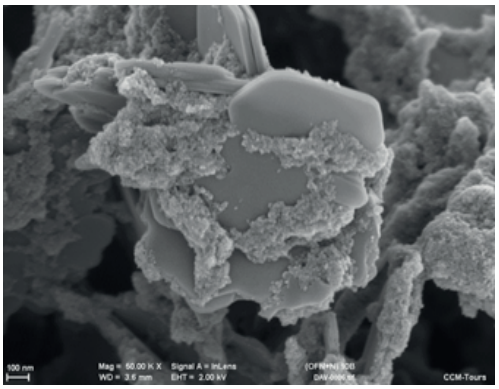 (b)

Fig. 10. SEM images of the products of transformation of naphthalene (a) and octafluoronaphthalene (b) in the contact layer region of the sample produced from a two-layer heterogeneous mixture $C_{10}H_8$ – $C_{10}F_8$ at 8 GPa and 1000 °C.

(Fig. 10b) presents a mixture of micron- and nano-size carbon states, graphite particles of ~1 μm size and aggregated nanoparticles of 10–15 nm size. SEM image of aggregated nanoparticles resembles the agglomerates of nanodiamonds. However, the HRTEM images of this material (Fig. 11) indicate that it is a combination of onion-like and polyhedral nanoparticles made up of several (2 to 5) closed graphene layers. The internal cavity of these nanoparticles contain disordered and low-ordered fractions of carbon.

Thus, the obtained results provide evidence for micron-size fractions of diamond formed in the products of thermal transformations of $C_{10}H_8$ – $C_{10}F_8$ binary mixtures under high pressures mainly from micron-size fractions of graphite, which are produced through carbonization of hydrocarbon and fluorocarbon compounds. For formation of nano-size fraction of diamond, carbon nanoparticles, produced by carbonization of fluorocarbon component of binary mixture, serve as a precursor.

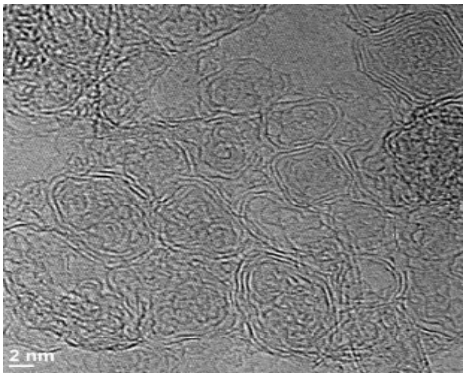

Fig. 11. HRTEM image of nano-size fraction of the products of octafluoronaphthalene transformation in the contact layer region of the sample produced by treatment of a two-layer heterogeneous mixture $C_{10}H_8$ – $C_{10}F_8$ at 8 GPa and 1000 °C.

6. HPHT synthesis of doped diamond

The demonstrated ability of producing diamonds in different size ranges through the catalyst-free HPHT transformations of mixtures of hydrocarbon and fluorocarbon compounds has also facilitated an ongoing research on synthesis under high static pressures of free from metal impurities diamonds doped with nitrogen and silicon atoms. These diamonds, particularly nanosize ones, possess high photoluminescence properties due to N-V and Si-V optical centers, making them suitable for applications as unbleached intracellular tags (or markers) [17]. To achieve this goal, a series of diamonds with several different doping contents of nitrogen and silicon have been synthesized by using the systems comprised of mixtures of hydrocarbons and fluorocarbons with N and Si – containing organic compounds [18, 19]. Detailed studies of optical properties of synthesized diamonds have proven that the proposed HPHT chemistry approach can indeed produce diamonds doped with high contents of different dopants. As an example, Fig. 12 presents a fluorescence and SEM microscopy images of the N-doped micro- and nanodiamond samples, synthesized in the system comprised of fluorographite-naphthalene-hexamethylenetetramine $C_6H_{12}N_4$ [18]. Taking into account that fluorescent properties of diamond are controlled mainly by abundance of N-V optical centers in the sample, this opens an opportunity for synthesis of samples possessing a very bright fluorescence considerably exceeding that of "detonation" nanodiamonds.

Si-doped diamonds have been recently synthesized by using a mixture of fluorographite and naphthalene at 1:1 molar ratio with the addition of variable contents of tetrakis(trimethylsilyl) silane $C_{12}H_{36}Si_5$ as a silicon source [19].

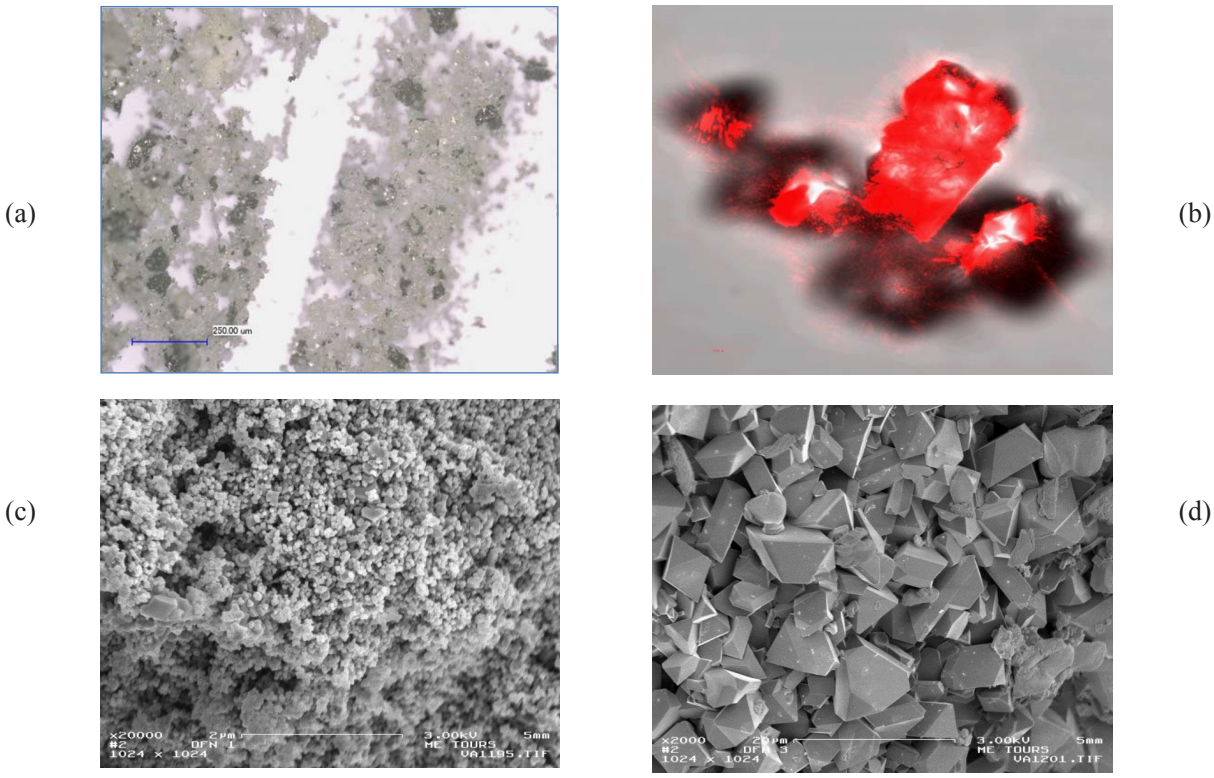

Fig. 12. Images of N-Doped Nano- and Microcrystalline Diamonds Produced From Mixture of Fluorinated Graphite-Naphthalene-Hexamethylenetetramine treated at 1000 °C for 20 sec at 8 GPa: (a) optical microscope image, (b) fluorescent microscopy image excited by 546 nm light; SEM images of nanocrystalline (c) and microcrystalline (d) diamonds.

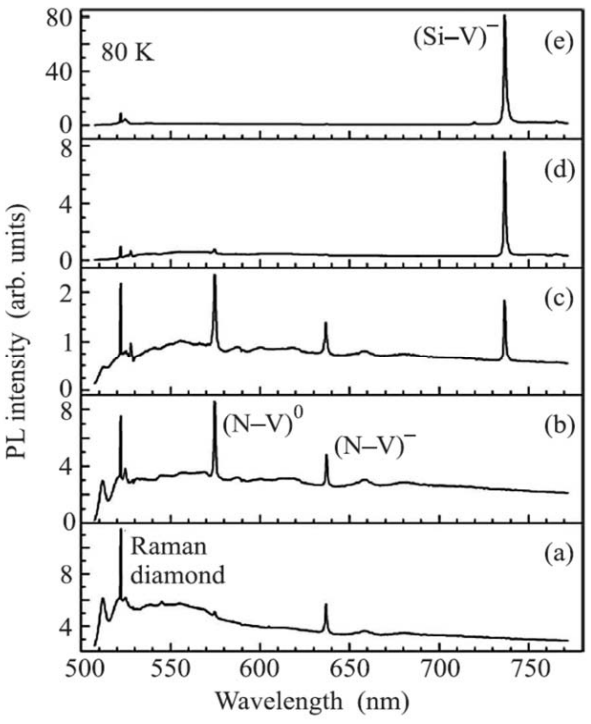

Fig. 13. Photoluminescence and Raman spectra of diamond samples produced by HPHT treatment from pure naphthalene (a), homogeneous mixture of $C_{10}H_8$ – C_1F_1 (b), and ternary mixtures $C_{10}H_8$ – C_1F_1 – $C_{12}H_{36}Si_5$ with variable Si/C atomic ratios 0.02 (c), 0.04 (d) and 0.07 (e).

Photoluminescence spectra (Fig. 13) of produced diamond samples show clear dependence on the composition of initial mixture.

In the photoluminescence spectra of samples produced without adding a Si-dopant, besides the intense Raman line of diamond at 522 nm (1332 cm^{-1}), a narrow bands at 575.1 and 637.5 nm were detected (Fig. 13a and b). They belong to neutral, (N-V)°, and negative, $(N\text{-}V)^-$, optical centers, respectively, which originate from defects appearing in diamond crystals produced by HPHT treatment of naphthalene-based pellets containing some atmospheric nitrogen adsorbed on the surface. In comparison, the spectra of diamond samples obtained from ternary mixtures $C_{10}H_8$ – C_1F_1 – $C_{12}H_{36}Si_5$ show a new sharp band at 737 nm which has grown in intensity with the increase in Si/C atomic ratios in the mixture (Fig. 13c-e). This band is mainly due to a zero-phonon line from luminescence of negatively charged $(Si\text{-}V)^-$ defects, content of which in diamond was found to grow with the increase of concentration of $C_{12}H_{36}Si_5$ compound in the mixture. The follow up studies [20] of optical properties of HPHT synthesized Si-doped nanodiamonds have revealed an unprecedented narrow optical transitions for individ-

ual colour centers in the crystals smaller than 200 nm. Individual spectral lines measured in photoluminescence excitation and corrected for apparent spectral diffusion yielded a homogeneous linewidth of about 200 MHz which is close to the lifetime limit. These results indicate the high crystalline quality achieved in these nanodiamond samples, and advance the applicability of nanodiamond-hosted colour centres for quantum optics applications.

7. Conclusions

The presented results clearly show that thermal decomposition of fluorinated graphite $CF_{1.1}$ under pressure of 8 GPa produces at temperature of 1000 °C graphite crystals which have a unique clear-cut hexagonal faces. The results also demonstrate a method developed for high pressure catalyst-free synthesis of high purity nano- and micronsize diamonds from hydrocarbon/fluorocarbon mixtures under heating at 900–1000 °C at 8 GPa, This method is unique since (i) it uses a mixture of solid hydrocarbons with fluorocarbons as precursors in absence of any catalysts and reduces by 300–400 °C the temperature of diamond synthesis as compared to pure hydrocarbon precursors, (ii) produces high yields of well-faceted nanosize (9–100 nm) along with a micronsize (0.3–13 μm) diamond crystals of high purity, shown by very low ash content (0.1 ± 0.05 wt.%). Method also opens an opportunity, as shown in case of N-doped and Si-doped diamonds, for synthesis of metal impurity free samples possessing a very bright fluorescence in high demand for biomedical imaging applications as a non-toxic carbon tags or markers and for application as a single photon emitters in quantum optics.

Acknowledgement

This work has been supported by the Russian Fund for Basic Research (grant N 15-03-04490) and US Civilian Research and Development Foundation (grant RUE2-2894-TI-07).

References

[1]. Hugh O. Pierson, Handbook of Carbon, Graphite, Diamond and Fullerenes. Properties and Applications, Noyes Publications, Park Ridge, New Jersey, USA. 1993. ISBN 0-8155-1339-9

[2]. Synthetic Diamond Market – Global Industry Analysis, Size, Share, Growth, Trends and Forecast 2015–2023. Transparency Market Research. Press Release. Published date: 2015-12-07.

[3]. F.P. Bundy, J. Chem. Phys. 38 (1963) 631–643. DOI: 10.1063/1.1733716

[4]. L.F. Vereschagin, O.N. Ryabinin, A.A. Semerchan, L.D. Lifshits, B.P. Demyashkevich, and S.V. Popova, Doklady AN SSSR, 11:78 (1972).

[5]. J.E. Dahl, S.G. Liu, and R.M.K. Carlson, Science 299 (2003) 96–99. DOI: 10.1126/science.1078239

[6]. R.H. Wentorf, J. Phys. Chem. 69 (1965) 3063–3069. DOI: 10.1021/j100893a041

[7]. E.N. Yakovlev, and O.A. Voronov, *Almazy i sverhtvjordye materialy* [Diamonds and ultrahard materials] 7 (1982) 1–2 (in Russian).

[8]. O.A. Voronov, V.V. Gavrilov, V.M. Zhulin, A.V. Rakhmanina, E.P. Khlybov, and E.N. Yakovlev, Doklady AN SSSR, 274:100 (1984).

[9]. O.A. Voronov, and A.V. Rakhmanina, *Neorganicheskie materialy* [Inorganic Materials] 28:1408 (1992) (in Russian).

[10]. V.A. Davydov, L.S. Kashevarova, and O.G. Revin, Russ. J. Phys. Chem. 70 (1996) 1012–1015.

[11]. V.A. Davydov, A.V. Rakhmanina, V. Agafonov, B. Narymbetov, J.-P. Boudou, and H. Szwarc, Carbon 42 (2004) 261–269. DOI: 10.1016/j.carbon.2003.10.026

[12]. V.A. Davydov, A.V. Rakhmanina, V. Agafonov, and V.N. Khabashesku, J. Phys. Chem. C, 115 (2011) 21000–21008. DOI:10.1021/jp206904t

[13]. V.A. Davydov, A.V. Rakhmanina, V. Agafonov, and V.N. Khabashesku, Nanosystems: physics, chemistry, mathematics 5 (1) (2014) 167–171.

[14]. V.A. Davydov, A.V. Rakhmanina, V. Agafonov, and V.N. Khabashesku, Carbon 90 (2015) 231–233. DOI: 10.1016/j.carbon.2015.03.055

[15]. V.A. Davydov, V. Agafonov, and V.N. Khabashesku, J. Phys. Chem. C 120 (51) (2016) 29498–29509: DOI 10.1021/acs.jpcc.6b10805.

[16]. W.R.L. Lambrecht, C.H. Lee, B. Segall, J. C. Angus, Z. Li, and M. Sunkara, Nature 364 (1993) 607–610. DOI:10.1038/364607a0

[17]. V. Vaijayanthimala, H.C. Chang, Nanomedicine 4 (2009) 47–55. DOI: 10.2217/17435889.4.1.47

[18]. V.A. Davydov, A.V. Rakhmanina and V.N. Khabashesku, US Patent No. 8945301, Issued on February 3, 2015.

[19]. V.A. Davydov, A.V. Rakhmanina, S.G. Lyapin, I.D. Il'ichev, K.N. Boldyrev, A.A. Shiryaev, and V. Agafonov, JETP Letters 99 (2014) 585–589. DOI: 10.1134/S002136401410004X

[20]. U. Jantzen, A.B. Kurz, D.S. Rudnicki, C. Schäfermeier, K.D. Jahnke, U.L. Andersen, V.A. Davydov, V.N. Agafonov, A. Kubanek, L.J. Rogers, and F. Jelezko, New Journal of Physics 18 (2016) 073036. DOI: 10.1088/1367-2630/18/7/073036